

Tight-binding approach to excitons bound to monolayer impurity planes: Strong radiative properties of InAs in GaAs

Rita Claudia Iotti and Lucio Claudio Andreani

INFN-Dipartimento di Fisica "Alessandro Volta," Università di Pavia, via Bassi 6, I-27100 Pavia, Italy

Massimiliano Di Ventura*

*Institut de Physique Appliquée, Ecole Polytechnique Fédérale, CH-1015 Lausanne, Switzerland
and Department of Physics and Astronomy, Vanderbilt University, Nashville, Tennessee 37235*

(Received 10 April 1998)

A theory of Wannier-Mott excitons bound to monolayer (ML) impurity planes in semiconductors, which is based on Green's function tight-binding calculations of the single-particle states, is presented. Binding energies and oscillator strengths for one and two MLs of InAs in GaAs are predicted to be much larger than in the usual $\text{In}_x\text{Ga}_{1-x}\text{As}/\text{GaAs}$ thick quantum wells. The reason is the increase of effective mass of both carriers due to folding of the InAs bands along the growth direction. The results suggest that ML insertions can be used as intense light sources in light-emitting devices.

[S0163-1829(98)51024-7]

Among the basic reasons of interest in spatially confined excitons are their increased binding energy (implying higher stability at room temperature) and oscillator strength (leading to a more efficient coupling with light). For excitons in quantum wells (QWs) both quantities reach a maximum at a critical well thickness, when carriers start to leak into the barriers.¹ Increasing the maximum values, thus giving strong radiative properties to the exciton, would be quite important, also for possible applications in light-emitting devices.

In this work we predict that binding energies and oscillator strengths much larger than corresponding QW values can be achieved for excitons bound to monolayer (ML) impurity planes, like, e.g., InAs in GaAs, which is the system considered here. This originates from folding of the bands of the impurity material along the growth direction, resulting in a large effective mass of both carriers. This effect goes beyond commonly adopted envelope-function (EF) models, and is derived here from a new approach to spatially confined excitons, which starts from tight-binding (TB) calculations of single-particle states.

The presence of an isovalent impurity plane (also called δ layer) in a bulk host matrix, like, e.g., In in GaAs or AlGaAs, or Ga in AlGaAs, gives rise to intense luminescence from excitons bound to the δ -layer.²⁻⁵ The strong excitonic properties of δ layers have not been theoretically explained up to now. Monolayer (and submonolayer) impurity planes represent the ultimate limit of narrow QWs: however since the bound levels are close to the band edges of the host, and several tenths of an eV far from those of the impurity material, an EF description of the ML impurity plane is inapplicable, raising a challenging theoretical problem.

Calculations of electronic states for InAs impurity layers in GaAs have been performed by TB (Refs. 6-9) as well as pseudopotential^{10,11} techniques. These approaches take into account the band structure features, at the atomic scale, of host and perturbing materials. Unlike EF schemes, they yield the band dispersion throughout the Brillouin zone, and make no assumptions about wave-function matching conditions at

the interfaces. The isovalent impurity plane produces an attractive short-range perturbation for both electron and heavy-hole levels, which always has a bound state, due to the one-dimensional (1D) nature of the density of states for a given in-plane wave vector (contrary to single isovalent impurities, for which a bound state occurs only if the short-range potential exceeds a certain threshold^{12,13}). Concerning exciton states bound to δ layers, the only previous atomic-scale approach consists of the linear-chain TB model of Ref. 2. Clearly it is highly desirable to have a formulation of the excitonic problem which starts from the electronic structure and is able to calculate exciton wave functions and oscillator strengths.

The present approach is based on the Green's function TB scheme of Ref. 9. We exploit the fact that the exciton is still Wannier-Mott-like, as far as the in-plane dynamics is concerned. The relative electron-hole radius in the plane is, in fact, much larger than the lattice constant, thereby permitting a shallow-exciton approximation for the in-plane motion only. The electron and hole dynamics along the growth direction is treated, instead, by the TB method: thus the effect of band folding along the growth direction is fully taken into account. We consider here the case of one and two MLs of InAs in GaAs.

The N -electron exciton wave-function is written as¹⁴

$$\Psi_{\text{exc}} = \sum_{c,v} \sum_{\mathbf{k}_c, \mathbf{k}_v} A_{cv}(\mathbf{k}_c, \mathbf{k}_v) \Phi_{v\mathbf{k}_v \rightarrow c\mathbf{k}_c}(\mathbf{r}_1, \dots, \mathbf{r}_N), \quad (1)$$

where $\mathbf{k}_c, \mathbf{k}_v$ are two-dimensional (2D) Bloch vectors for the crystal with the impurity plane, c (v) is a conduction- (valence-) band index which may have a discrete and a continuous part, and $\Phi_{v\mathbf{k}_v \rightarrow c\mathbf{k}_c}$ is a Slater determinant obtained from the Hartree-Fock ground state by replacing the valence Bloch function $\psi_{v\mathbf{k}_v}$ with the conduction one $\psi_{c\mathbf{k}_c}$. Spin indexes are understood. The \mathbf{k} -space equation for the envelope function $A_{cv}(\mathbf{k}_c, \mathbf{k}_v)$ has the usual form,¹⁴ but here all wave

vectors are in 2D. The Coulombic matrix element can be evaluated by expanding the products of periodic parts $u_{c\mathbf{k}}$, $u_{v\mathbf{k}}$ of the Bloch functions in plane waves with reciprocal lattice vectors:

$$u_{c\mathbf{k}_c}^*(\mathbf{r})u_{c'\mathbf{k}'}(\mathbf{r}) = \sum_{\mathbf{G}} C(c\mathbf{k}_c, c'\mathbf{k}'; \mathbf{G}) e^{i\mathbf{G}\cdot\mathbf{r}}, \quad (2)$$

and similarly for the valence Bloch functions.

We consider only optically active exciton states, i.e., with

$$[\epsilon_c(\mathbf{k}) - \epsilon_v(\mathbf{k}) - E]A_{cv}(\mathbf{k}) - \sum_{c'v'\mathbf{k}'} \frac{2\pi e^2}{\epsilon|\mathbf{k}-\mathbf{k}'|} A_{c'v'}(\mathbf{k}') \int \int_{-\infty}^{+\infty} C(cc'; z_1) C^*(vv'; z_2) e^{-|\mathbf{k}-\mathbf{k}'||z_1-z_2|} dz_1 dz_2 = 0, \quad (3)$$

where $\epsilon_c(\mathbf{k}_c)$ [$\epsilon_v(\mathbf{k}_v)$] is the conduction- (valence-) band dispersion, ϵ is the background dielectric constant, and

$$C(cc'; z) = \int_{cell} u_{c0}^*(\vec{\rho}, z) u_{c'0}(\vec{\rho}, z) d\boldsymbol{\rho} \quad (4)$$

is the planar cell average of the product of zone-center Bloch functions. We emphasize that the full conduction and valence-band dispersion is retained in Eq. (3): no effective-mass approximation is made.

The wave functions are calculated in the TB Green's function formalism. The host crystal is described by a TB Hamiltonian H^0 in the basis of sp^3s^* atomiclike orthogonal orbitals centered on each atomic site.¹⁵ Spin and strain have been consistently included.⁹ The retarded Green's function matrix G^0 of the host material is represented in a basis which is Bloch-like in the plane parallel to the impurity layer and Wannier-like perpendicular to it.⁶ It is related to the TB atomiclike basis by a unitary transformation and can be written as (we refer to the [001] direction, which is the one relevant for this work),

$$|\mathbf{k}lj\rangle = \frac{1}{\sqrt{N_z}} \sum_{\mathbf{k}_z} e^{-i\mathbf{k}_z \cdot \mathbf{R}_j} |\mathbf{k} + \mathbf{k}_z, l\rangle \quad (5)$$

where $l = s, p_x, p_y, p_z, s^*$, \mathbf{k} is a 2D Bloch vector, j indexes the layers, \mathbf{R}_j is any lattice vector of layer j , \mathbf{k}_z is a wave vector along [001], and N_z is the number of layer planes considered. The perturbation induced by the impurity layer is then constructed according to the prescriptions of Refs. 8 and 9. The parameters of InAs and GaAs have been chosen in order to reproduce the gaps at the critical points *and* the electron and hole effective masses at Γ .¹⁶ Strain of the InAs layer is included by scaling the TB parameters in order to reproduce the relevant deformation potentials. More details can be found in Ref. 9, where the parametrization of InAs is also given. Measuring energies from the valence-band top of GaAs, the heavy-hole (HH) and conduction-band (CB) levels are bound at 23 and 1468 meV for 1 ML, respectively, and at 54 and 1406 meV for 2MLs. The corresponding localization energies of CB measured from the bottom of the conduction band of GaAs are then 52 meV for 1 ML and 114 meV for 2 MLs.

$\mathbf{k}_c = \mathbf{k}_v \equiv \mathbf{k}$. The shallow (Wannier-Mott) exciton approximation for the in-plane dynamics is defined by keeping only the $\mathbf{G} = \mathbf{0}$ term in Eq. (2), and by neglecting the (small) variation of $u_{c\mathbf{k}}, u_{v\mathbf{k}}$, when the 2D wave vector varies on the scale of the inverse exciton radius. These approximations will be justified *a posteriori*, as usual,¹⁴ by verifying that the envelope function $A(\mathbf{k}, \mathbf{k}) \equiv A(\mathbf{k})$ is strongly peaked around $\mathbf{k} = \mathbf{0}$. The \mathbf{k} -space equation (omitting the exchange interaction) becomes

The indexes c, v in Eq. (3) run over the discrete (bound) and continuum (unbound) states of the ML impurity plane. In the strong confinement regime for the exciton, when there is separate quantization of electron and hole levels, the exciton wave function is well represented by keeping only the electronic states bound to the ML. The linear-chain model of Ref. 2 indicates that the projection of the exciton onto the separable wave-function, obtained by keeping only the bound state, is as high as 99% for 1 ML InAs in GaAs: thus separate electron and hole localization applies. A similar conclusion is also suggested by EF calculations.¹⁷ Thus we make the approximation of keeping only the bound conduction and valence states in Eq. (3). The continuum part of the spectrum needs to be included in order to describe submonolayers of InAs in GaAs, where a crossover to weak (center of mass) confinement regime is expected to occur.¹⁷

We make an axial approximation for the in-plane dispersion of both electron and hole. The integral equations (3) are solved by the modified quadrature method:¹⁸ the wave vector variable is discretized according to a Gaussian formula, while a singular function is added and subtracted in order to remove the divergence of the Coulomb potential, and the resulting matrix is diagonalized numerically. The oscillator strength is calculated as

$$f_\epsilon = \frac{2}{m_0 \hbar \omega} \left| \sum_{cv} \langle u_{c0} | \boldsymbol{\epsilon} \cdot \mathbf{p} | u_{v0} \rangle \sum_{\mathbf{k}} A_{cv}(\mathbf{k}) \right|^2. \quad (6)$$

The momentum matrix element between Bloch functions is assumed to be given by its bulk value $2|\langle u_{c0} | \mathbf{p} | u_{v0} \rangle|^2/m_0 = 25.7$ eV times an electron-hole overlap integral.

The empirical TB scheme yields the planar average of Bloch functions for each atomic layer. A further average in the growth direction has been performed in order to eliminate the oscillations between anionic and cationic layers. The result is the analog of the macroscopic average used in band-offset calculations.¹⁹ This average TB wave function can be compared to the result of the usual EF scheme. In Fig. 1 we show the probability density of CB and HH levels for 1ML of InAs in GaAs, calculated by the TB and EF.²⁰ The electron level is more localized in the TB than in the EF calculation, due to the larger localization energy (the EF yields a CB localization energy of 22 meV for 1ML, and 77 meV for

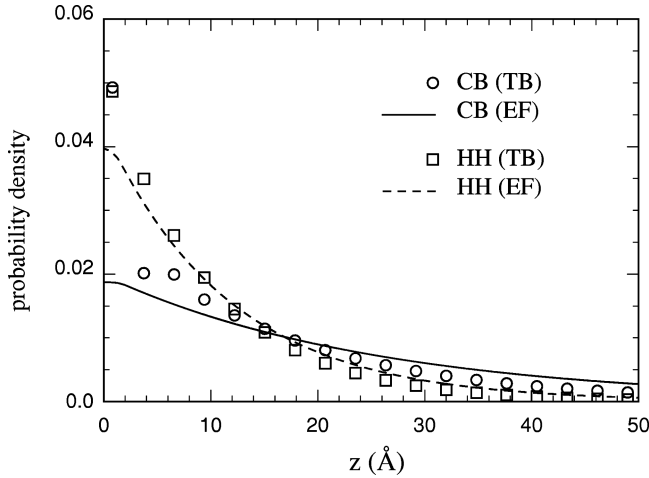


FIG. 1. Electron and hole probability densities along the growth direction for 1 ML InAs in GaAs. Circles/squares: TB calculation. Full/dashed lines: EF scheme.

2 MLs). On the other hand the probability density of the HH level is similar in TB and EF schemes.

The 2D dispersion of the bound levels is crucial for excitonic properties. The in-plane effective masses (in units m_0) are found to be $m_e=0.079$, $m_h=0.361$ for 1 ML; $m_e=0.093$, $m_h=0.305$ for 2 MLs. The effective masses are *larger* than the bulk GaAs values.²⁰ This is contrary to expectations from EF models, which would lead to in-plane masses intermediate between those of GaAs and InAs. The different TB results are due to the fact that the CB and HH confined levels are far from the band edges of InAs: thus the ‘‘effective masses’’ of the InAs layer are much higher than their values at the Γ point. In other words, *folding of the InAs bands along the growth direction leads to a sizeable increase of the 2D effective mass for the ML impurity*. Actually the in-plane dispersion of both CB and HH is strongly nonparabolic: the full dispersion has been used in the exciton calculation.

In Fig. 2 we show the k -space exciton envelope function $A(k)$ for one and two MLs. It can be seen that $A(k)$ decays at wave vectors of the order of $0.01 \times 10^8 \text{ cm}^{-1}$: thus the shallow-exciton approximation discussed above is very well

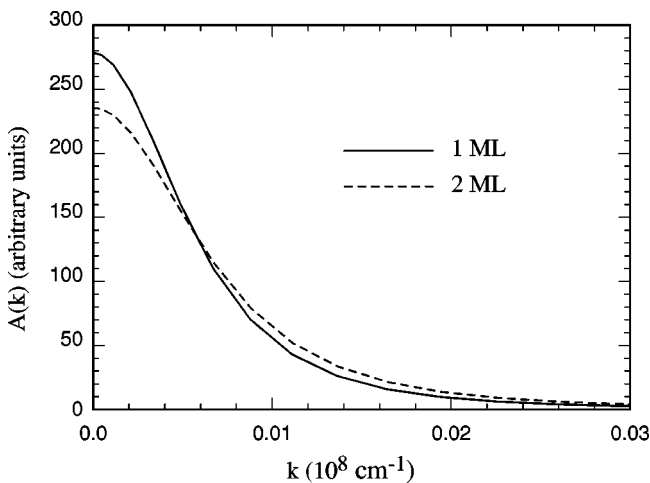


FIG. 2. In-plane exciton envelope function for one and two MLs of InAs in GaAs.

TABLE I. Binding energies (in meV) and oscillator strengths per unit area for in-plane polarization (10^{12} cm^{-2}) for the HH-CB exciton for one and two MLs of InAs in GaAs.

	E_b	f
1 ML	12.9	12.9
2 MLs	15.7	19.5

justified. The envelope function for two MLs is more extended in k space (therefore more localized in real space) than for one ML: this is due to the stronger localization of single-particle levels for 2 MLs.

In Table I we present our results for 1 and 2 MLs of InAs in GaAs. Binding energies and oscillator strengths increase with the number of layer insertions: this is a further indication that the exciton is in strong-confinement regime. The TB results are much larger than in $\text{In}_x\text{Ga}_{1-x}\text{As}/\text{GaAs}$ QWs (where typical values are $E_b \sim 8 \text{ meV}$ and $f \sim 4 \times 10^{12} \text{ cm}^{-2}$);¹⁷ the oscillator strengths for 1 ML and 2 MLs are larger by a factor of 3 to 5. This implies that the probability of photon absorption by a single InAs ML in GaAs is larger than for a $\text{In}_x\text{Ga}_{1-x}\text{As}/\text{GaAs}$ QW of, say, 80-Å width. The enhanced excitonic effect is due to a combination of different factors: increased wave function localization (see Fig. 1), large in-plane masses, and in-plane nonparabolicity, all go in the direction of *increasing* binding energies and oscillator strengths.

We now discuss the approximations made. The effect of single-particle continuum has been estimated by comparing k -space EF results with those of a real-space EF approach, which includes all bound and continuum levels.¹⁷ The electron and hole continuum gives a negligible effect on the binding energies, but it increases the oscillator strengths by 27% (for 1 ML) or 10% (for 2 MLs). The momentum matrix element shows little variation among III-V semiconductors: from $\mathbf{k} \cdot \mathbf{p}$ theory,²¹ its value for the ML impurity is expected to be inversely proportional to the in-plane effective mass, and therefore it should be decreased with respect to the GaAs value by a factor of the order of 10–30%. The use of the GaAs dielectric constant in Eq. (3) has been tested by evaluating the effect of image charges in the real-space EF approach¹⁷: the effect is found to be smaller than a percent. q -dependent screening is usually negligible for large-radius excitons. Finally, in order to investigate the dependence on TB parametrization we have repeated the calculation for 1 ML using the TB parameters of Ref. 5. Binding energies (oscillator strengths) turned out to be smaller by about 20% (40%), mainly due to a smaller electron localization energy; the in-plane dispersion is almost unchanged. The different results for the two parametrizations follow from the inability of knowing and reproducing the bulk band structure with sufficient accuracy. Our tests indicate that the results are most sensitive to the GaAs masses at the Γ point, and to the InAs band dispersion along the [001] direction at wave vectors $\sim 0.2 \times 2\pi/a$ (where a is the lattice constant): at such wave vectors the two parametrized bulk bands differ only by a fraction of an eV. Even within the quoted uncertainties, the resulting binding energies and oscillator strengths are much higher than in $\text{In}_x\text{Ga}_{1-x}\text{As}/\text{GaAs}$ QWs, and the previous conclusions about the role of band folding are valid.

Several experimental investigations of MLs and sub-MLs of InAs in GaAs have been published²⁻⁵ (a more complete list can be found in Refs. 5 and 9), but no determinations of exciton binding energies have been reported. The observed strong radiative properties point towards high values for the oscillator strengths,²⁻⁴ which, however, cannot be quantitatively measured by the commonly employed photoluminescence and photoluminescence excitation techniques. The transmission experiment of Ref. 3 on a GaAs sample containing one 0.5 ML insertion of InAs yields a strong dip associated with the localized exciton: this indicates that the oscillator strength is much larger than in QWs, where the change in transmission due to a single QW is barely visible. The present results call for systematic measurements of binding energies and oscillator strengths for excitons bound to ML insertions.

We now briefly discuss possible implications of our results. An exciton binding energy in excess of 12 meV (which is comparable to values for GaAs/Al_xGa_{1-x}As QWs) implies that excitonic effects could be observable at room temperature. In addition to applications in usual QW-like structures,

the large values for the oscillator strength suggest that InAs monolayers could be usefully employed as the active medium in GaAs-based microcavities.²² The Rabi splitting is expected to be larger than in microcavities with embedded QWs, because of both the larger oscillator strengths *per ML* as well as the number of uncoupled MLs which can be inserted. Achieving a sizable Rabi splitting at room temperature would make microcavities with embedded MLs quite attractive for application in VCSELs and other optical devices.

Note added. A recent publication²³ reports on the observation of highly efficient laser emission from a single 1.5-ML-thick InAs layer in bulk GaAs, and gives evidence for the excitonic character of the recombination. This result confirms the importance of excitonic effects for InAs MLs in GaAs.

It is a pleasure to acknowledge fruitful discussions with A. Bitz, R. Colombelli, and J.-L. Staehli. One of us (R.C.I.) is grateful to EPFL for its hospitality to her during the course of this work.

*Electronic address: diventra@dynix.phy.vanderbilt.edu

¹R. L. Greene, K. K. Bajaj, and D. E. Phelps, Phys. Rev. B **29**, 1807 (1984).

²R. Cingolani *et al.*, Phys. Rev. B **42**, 3209 (1990); O. Brandt, H. Lage, and K. Ploog, *ibid.* **43**, 14 285 (1991).

³R. Schwabe *et al.*, J. Appl. Phys. **77**, 6295 (1995).

⁴M. V. Belousov *et al.*, Phys. Rev. B **51**, 14 346 (1995).

⁵R. Colombelli *et al.*, Appl. Phys. Lett. **68**, 1534 (1996).

⁶H. P. Hjalmarson, J. Vac. Sci. Technol. **21**, 524 (1982).

⁷S. Wilke and D. Hennig, Phys. Rev. B **43**, 12 470 (1991).

⁸K. A. Mäder and A. Baldereschi, in *Optics of Excitons in Confined Systems*, edited by A. D'Andrea *et al.* (IOP, Bristol, 1992), p. 341.

⁹M. Di Ventra and K. A. Mäder, Phys. Rev. B **55**, 13 148 (1997). There is a misprint in the spin-orbit parameters of InAs reported in this paper. The correct values (in eV) are $\lambda_a=0.1385$, $\lambda_c=0.129$.

¹⁰K. Shiraishi and E. Yamaguchi, Phys. Rev. B **42**, 3064 (1990).

¹¹J. E. Bernard and A. Zunger, Appl. Phys. Lett. **65**, 165 (1994).

¹²R. A. Faulkner, Phys. Rev. **175**, 991 (1968).

¹³A. Baldereschi and J. J. Hopfield, Phys. Rev. Lett. **28**, 171 (1972); A. Baldereschi, J. Lumin. **7**, 79 (1973).

¹⁴F. Bassani and G. Pastori Parravicini, *Electronic States and Optical Transitions in Solids* (Pergamon, Oxford, 1975).

¹⁵P. Vogl, H. P. Hjalmarson, and J. D. Dow, J. Phys. Chem. Solids **44**, 365 (1983).

¹⁶We used the following parameters for GaAs (all energies are in eV and the notation is the same as in Ref. 15): $E(s,a)=-8.1734$, $E(p,a)=0.9275$, $E(s^*,a)=8.4775$, $E(s,c)=-2.7738$, $E(p,c)=3.5547$, $E(s^*,c)=6.6247$, $V_{ss}=-6.4513$, $V_{xx}=1.9546$, $V_{xy}=4.77$, $V(sa,pc)=4.48$, $V(sc,pa)=7.85$, $V(s^*a,pc)=4.8422$, $V(s^*c,pa)=7$, $\lambda_a=0.13$, $\lambda_c=0.058$. The resulting electron, heavy-hole, and light-hole masses at Γ along [001] are (in units of free electron mass m_0) $m_e=0.070$, $m_{hh}=0.470$, and $m_{lh}=0.073$, respectively. The gap is 1.52 eV.

¹⁷R. C. Iotti and L. C. Andreani, Phys. Rev. B **56**, 3922 (1997).

¹⁸C. Y. P. Chao and S. L. Chuang, Phys. Rev. B **43**, 6530 (1991); R. Winkler, *ibid.* **51**, 14 395 (1995).

¹⁹A. Baldereschi, S. Baroni, and R. Resta, Phys. Rev. Lett. **61**, 734 (1988).

²⁰The conduction and valence band offsets used in the EF approximation are 0.716 eV and 0.278 eV, respectively. The electron effective mass (in units of m_0) has been assumed 0.067 in GaAs and 0.023 in InAs. The heavy-hole effective mass along [001] is 0.377 for GaAs and 0.341 for InAs.

²¹P. Y. Yu and M. Cardona, *Fundamentals of Semiconductors* (Springer, Berlin, 1996).

²²C. Weisbuch *et al.*, Phys. Rev. Lett. **69**, 3314 (1992); R. Houdre *et al.*, Phys. Rev. B **49**, 16 761 (1994).

²³A. R. Goñi *et al.*, Appl. Phys. Lett. **72**, 1433 (1998).